Metal π-complexes of benzene derivatives
XLVIII [☆]. Dimethylphosphano derivatives of bis(benzene) chromium as monodentate and chelating ligands at μ-ethylidyne-nona(carbonyl)-tri(cobalt).
Synthesis via ETC-autocatalysis, crystal structure determination and redox behavior of $[(Me_2P-\eta^6-C_6H_5)(\eta^6-C_6H_6)Cr[(\mu-MeC)Co_3(CO)_8]$, $[(Me_2P-\eta^6-C_6H_5)_2Cr][(\mu-MeC)Co_3(CO)_8]_2$ and $[(Me_2P-\eta^6-C_6H_5)_2Cr][(\mu-MeC)Co_3(CO)_7]$

Christoph Elschenbroich [*], Thomas Isenburg, Andreas Behrendt, Gerlinde Frenzen,
Klaus Harms

Fachbereich Chemie der Philipps-Universität, Hans-Meerwein-Strasse, D-35032 Marburg, Germany

Received 10 April 1995

Abstract

Reaction of μ-ethylidyne-nona(carbonyl)-tri(cobalt) (3) with $(Me_2P-\eta^6-C_6H_5)(\eta^6-C_6H_6)Cr$ (1) and $(Me_2P-\eta^6-C_6H_5)_2Cr$ (2), respectively, at ambient temperature affords the substitution products $[(Me_2P-\eta^6-C_6H_5)(\eta^6-C_6H_6)Cr[(\mu-MeC)Co_3(CO)_8]$ (5), $[(Me_2P-\eta^6-C_6H_5)_2Cr][(\mu-MeC)Co_3(CO)_8]_2$ (6) and $[Me_2P-\eta^6-C_6H_5Cr][(\mu-MeC)Co_3(CO)_7]$ (7). The surprisingly mild conditions under which these reactions proceed are a consequence of an electron-transfer chain (ETC) autocatalysis which operates due to the close proximity of the redox potentials $1^{+/0}$, $2^{+/0}$ and $3^{0/-}$ as determined by cyclic voltammetry. In the case of 6, reduction of the two CCo$_3$ carbonyl cluster units does not feature redox splitting, i.e. $\delta E_{1/2} < 100$ mV. EPR evidence for the ETC mechanism, which is initiated by the formation of the radical ions $1^{+\cdot}$, $2^{+\cdot}$ and $3^{-\cdot}$, is also presented. Compounds 6 and 7 were subjected to X-ray diffraction analysis. 6: triclinic, $P\bar{1}$, $a = 862.5(4)$ pm, $b = 1005.7(5)$ pm, $c = 1282.7(3)$ pm, $\alpha = 106.54(3)°$, $\beta = 94.86(3)°$, $\gamma = 93.52(4)°$, $Z = 1$, $wR = 0.073$ for 2419 reflections with $F > 4\sigma(F)$. 7: triclinic; $P\bar{1}$, $a = 1047.4(2)$ pm, $b = 1068.0(1)$ pm, $c = 1442.4(2)$ pm, $\alpha = 90.36(1)°$, $\beta = 110.34(1)°$, $\gamma = 113.32(1)°$, $Z = 2$, $R = 0.0435$ for 2241 reflections with $F > 4\sigma(F)$.

Keywords: Chromium; Cobalt; π-Benzene complexes; μ_s-Ethylidyne; Structure

1. Introduction

Bis(arene)metal complexes and transition metal carbonyl clusters exhibit rich redox chemistries and, at times, structural consequences of electron transfer processes [2]. It therefore is interesting to unite both structural types in the same molecule and to investigate any cooperative effects, in particular, to gauge the extent to which the moieties interact, as demonstrated by possible

shifts and splittings of redox potentials [3] and by modification of hyperfine splitting patterns in the EPR spectra [1]. Since, as yet, access to functional derivatives of bis(arene)metals is widest for chromium as the central metal atom and the redox chemistry of alkylidyne-capped clusters (μ-RC)Co$_3$(CO)$_9$ has been investigated extensively [4], we decided to study the reaction of the organometallic ligands $(Me_2P-\eta^6-C_6H_5)(\eta^6-C_6H_6)Cr$ (1) and $(Me_2P-\eta^6-C_6H_5)_2Cr$ (2) [5] with (μ-MeC)Co$_3$(CO)$_9$ (3). Although similar studies dealing with bis(diphenylphosphano-η^5-cyclo-pentadienyl)iron (4) as an organometallic diphos-type ligand have already been performed [6], a parallel investigation

---

Fig. 1. (a) The molecular structure of compound 6 in the crystal; (b) stereoplot of the unit cell of 6.

using the bis(arene)metal based analog 2 is warranted since 2, is less bulky than 4 and, as a radical cation 2^{+}·, more stable than the ferricinium derivative 4^{+}· [6d]. Furthermore, the very similar potentials for the redox couples 2$^{+/0}$ and 3$^{0/-}$ suggest an interesting electronic situation in a sandwich-cluster composite formed from 2 and 3 via carbonyl substitution.

2. Results and discussion

2.1. Synthesis and structural characterization

Replacement of carbonyl ligands of the cluster 3 by the organometallic phosphanes 1 and 2 is surprisingly facile, proceeding readily at room temperature (Scheme 1). This contrasts with the reactions of the ferrocenylphosphane 4 in particular and organophosphanes in general which, in the absence of redox catalysts, require extended heating at 60°C. Selective formation of the bis cluster-substituted product 6 and the interannularly cluster-bridged chelate 7 is governed by stoichiometry and reaction conditions, a concentrated solution of the educts (3 : 2 = 2 : 1) leading to 6 and slow addition (3 : 2 = 1 : 1) under high dilution yielding 7. Whereas the complexes 6 and 7 are obtained in crystalline state, 5, like the phosphane complex (μ-MeC)Co$_3$(CO)$_8$-(PMe$_2$Ph) [7a], is formed as a dark violet oil.

The compounds 6 and 7 were subjected to X-ray diffraction; structural plots are presented in Figs. 1 and
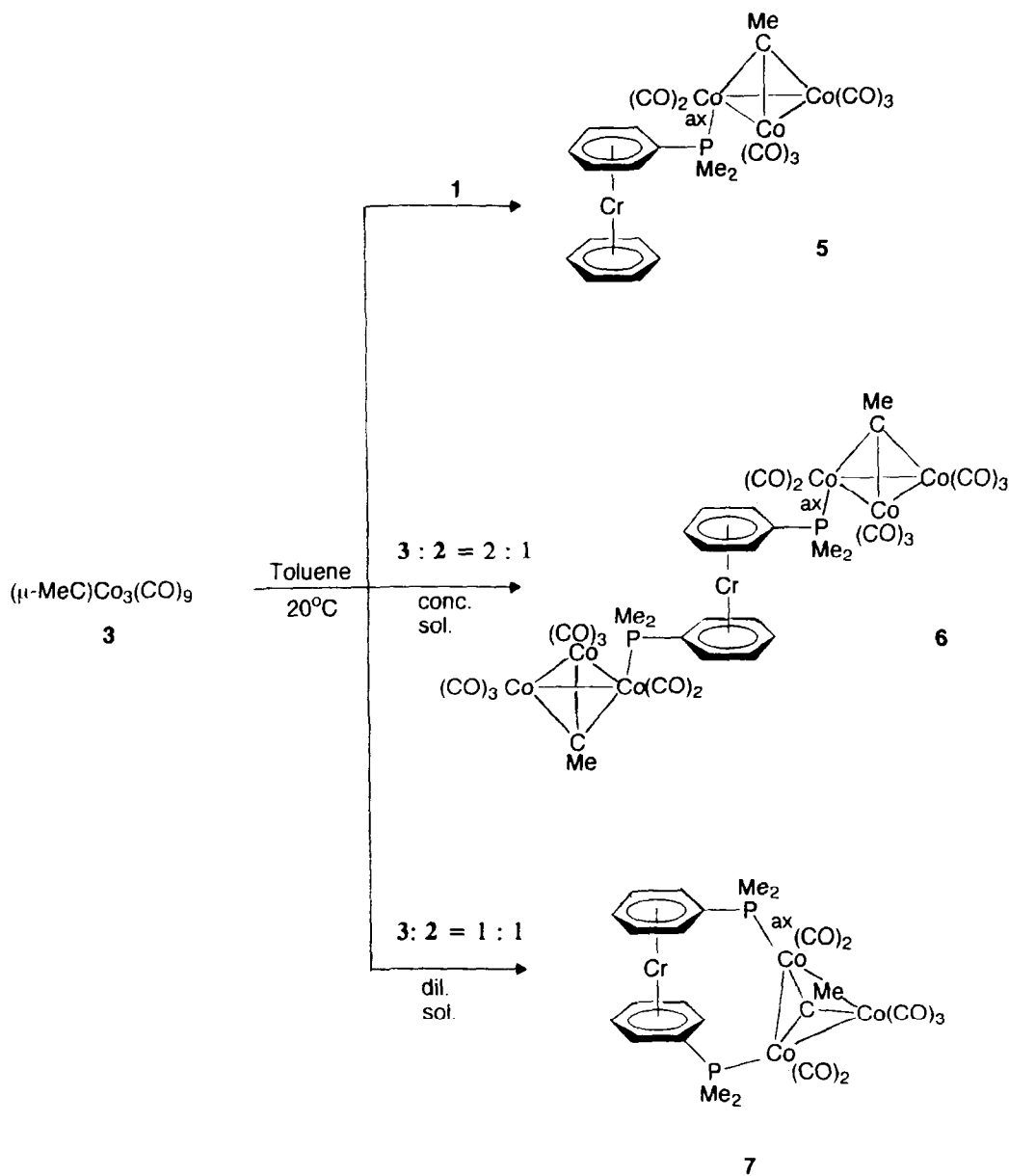
Scheme 1.

2, the relevant parameters are collected in Tables 1 and 2. The structure of 6 bears a strong resemblance to that of μ-[(Me$_2$P-η^6-C$_6$H$_5$)$_2$Cr][(η^5-MeC$_5$H$_4$)(CO)$_2$Mn]$_2$ (8) [8], featuring an antiperiplanar conformation of the central sandwich unit and a center of inversion. With regard to the coordinated (μ-MeC)Co$_3$(CO)$_8$ units, three aspects are worth mentioning: the geometrical preference (equatorial vs. axial); the coordination mode of the equatorial CO ligands (terminal vs. bridging); and the distortion of the CCo$_3$ frame. The criteria which determine whether an equatorial or an axial CO ligand at (μ-RC)Co$_3$(CO)$_9$ is displaced by a phosphane unit are far from clear and no simple predictive rule has been forthcoming. From an inspection of the literature it

appears that equatorial substitution is more abundant (examples: (μ-MeC)Co$_3$(CO)$_8$PPh$_3$ [7b], (μ-MeC) Co$_3$(CO)$_8$[P(OMe)$_3$]$_3$ [9], [(μ-PhC)Co$_3$-(CO)$_8$]$_2$Ph$_2$PC$_2$H$_4$PPh$_2$ [10], (μ-Me)Co$_3$-(CO)$_7$Ph$_2$PCH$_2$PPh$_2$ [11], [(μ-MeC)Co$_3$(CO)$_8$]$_2$-(Ph$_2$P-η^5-C$_5$H$_4$)$_2$Fe (9) [6b] and that axial substitution requires special circumstances like steric bulk of the ligand as in the complex (μ-PhC)Co$_3$(CO)$_8$P(cyhex)$_3$ [12]. There is, however, evidence that equatorial substitution reflects kinetic and axial substitution thermodynamic control, that both isomers may coexist in solution, and that equatorial-to-axial isomerization can be effected thermally [7,10,13]. The bis(arene)chromium derived ligand 2, in both its terminal (6) and chelating

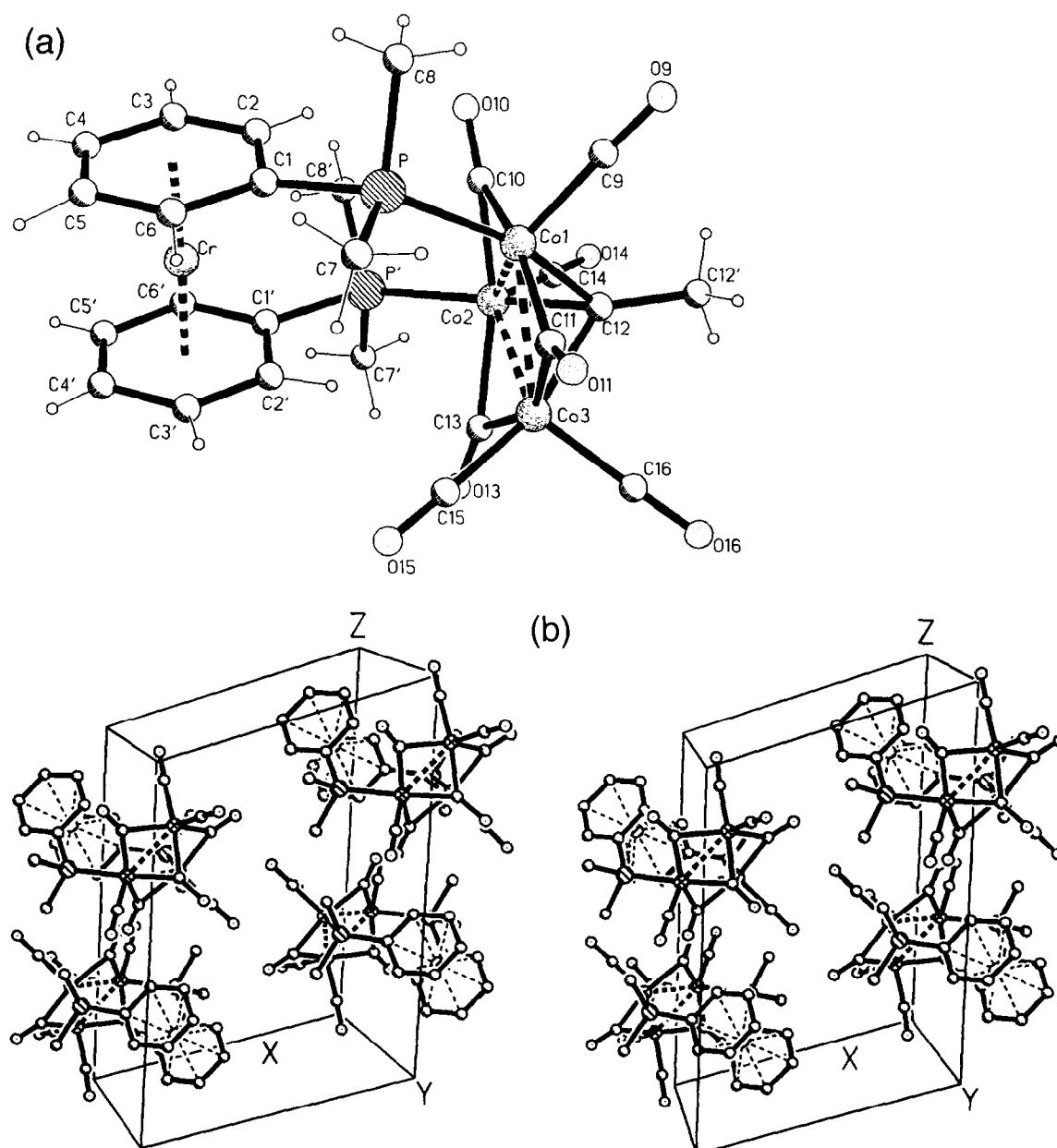Fig. 2. (a) The molecular structure of compound 7 in the crystal; (b) stereoplot of the unit cell of 7.

(7) modes at 3, engages in axial coordination. Whereas for the interannularly bridged complexes 7 and 10 the orientation is identical, it differs for the open derivatives in that 6 is axially and 9 is equatorially coordinated.

The situation is somewhat more transparent with regard to the CO bridging/nonbridging alternatives. It is generally accepted that with increasing σ-donor/π-acceptor ratio of the incoming phosphane, CO ligands at the (μ-RC)Co$_3$(CO)$_{9-n}$L$_n$ clusters move into bridging positions, in this way dissipating electron density more effectively [14]. Since the bis(η^6-arene)chromium unit, as implied by X-ray photoelectron spectroscopy [15a] and by the basicity of (H$_2$N-η^6-C$_6$H$_5$)$_2$Cr [15b], clearly is electron donating, it comes as no surprise that the structures of 6 and 7, like that of the ferrocene analog 10 [6a] exhibit equatorial CO bridging. The dimensions of the CCo$_3$ frame remain essentially unchanged, however, compared with those of the precursor 3 [14]. Note that in the chelate 7 the length of the bond Co(1)–Co(2), which is bridged by bidentate 2, does not differ from those of the unsupported bonds Co(2)–Co(3) and Co(3)–Co(1). This attests to the flexibility of diphos-type ligands which possess a bis(arene)metal backbone. Here, as well as for the ferrocene derived diphos ligands, two orthogonal degrees of freedom — rotations around the sandwich- and the C(π-perimeter)–P-bonds — ascertain that ligand geometry may adapt in an optimal way to the requirements of the metal–metal

bond to be spanned. In the case of complex 7 this is accomplished by a sandwich torsional angle centroid-C(1)–centroid'-C(1') of 57.3° which for the bis(arene)chromium unit preserves its favored eclipsed conformation.

The question as to the presence or absence of CO bridging may also be tackled by means of IR spectroscopy with the advantage that any changes of the coordination mode with changes in the state of aggregation are easily assessed. It has been demonstrated that bridging CO groups in the crystalline state may transform into terminal CO ligands in solution. With regard to the class of compounds treated in this paper, (μ-MeC)Co$_3$(CO)$_8$P(C$_6$H$_{11}$)$_3$ [16] represents a case in point. A comparison of the IR spectra of 6 and 7 in the solid and dissolved states is presented in Fig. 3. Whereas for the complex 7 the relative band intensities in the regions characteristic for terminal and bridging CO groups are only marginally affected, dissolution of 6 leads to a pronounced decrease of intensity in the μ-CO region (1800–1880 cm^{-1}). This finding ties in with the idea that CO bridging is favored by the incorporation of electron-donating ligands into the cluster: bridging and nonbridging modes are of similar energy for 6, which contains mono-substituted clusters, while they differ significantly for disubstituted 7. Consequently, for 7 the CO bridging mode is maintained even in solution while for 6 the bridges open up.

Table 1
Selected interatomic distances (pm) and bond angles (°) for 6

Cr(1)–C(1)	217.7(13)	C(7)–P	182.5(11)	Co(2)–C(13)	194.0(15)
Cr–C(2)	219.4(12)	C(8)–P	181.9(13)	Co(2)–C(14)	176.9(12)
Cr–C(3)	216.8(12)	Co(1)–P	227.2(4)	Co(2)–C(17)	180.8(12)
Cr–C(4)	217.2(12)	Co(1)–Co(2)	247.9(3)	Co(3)–C(11)	194.6(14)
Cr–C(5)	217.9(10)	Co(2)–Co(3)	245.8(2)	Co(3)–C(13)	199.9(14)
Cr–C(6)	219.4(11)	Co(3)–Co(1)	244.2(3)	Co(3)–C(15)	179.8(11)
C(1)–C(2)	146.4(18)	Co(1)–C(12)	190.7(13)	Co(3)–C(16)	177.9(14)
C(2)–C(3)	143.4(24)	Co(2)–C(12)	189.8(12)	C(9)–O(9)	115.0(19)
C(3)–C(4)	140.3(18)	Co(3)–C(12)	189.2(10)	C(10)–O(10)	115.0(16)
C(4)–C(5)	137.6(19)	Co(1)–C(9)	173.3(15)	C(11)–O(11)	117.0(17)
C(5)–C(6)	140.3(18)	Co(1)–C(10)	189.2(12)	C(13)–O(13)	114.9(20)
C(6)–C(1)	144.4(17)	Co(1)–C(11)	194.7(11)	C(14)–O(14)	113.4(14)
C(1)–P	177.0(14)	Co(2)–C(10)	204.1(15)	C(15)–O(15)	112.0(14)
				C(16)–O(16)	112.4(17)
C(6)–C(1)–C(2)	116.1(12)	Co(1)–Co(2)–Co(3)	59.3(1)		
C(1)–C(2)–C(3)	118.8(11)	Co(3)–Co(1)–Co(2)	59.9(1)		
C(2)–C(3)–C(4)	120.8(13)	Co(2)–Co(3)–Co(1)	60.8(1)		
C(3)–C(4)–C(5)	122.1(14)	Co(1)–C(10)–Co(2)	77.8(5)		
C(4)–C(5)–C(6)	118.4(11)	Co(1)–C(11)–Co(3)	77.7(4)		
C(5)–C(6)–C(1)	123.7(11)	Co(2)–C(13)–Co(3)	77.2(6)		
C(7)–P–C(8)	101.7(5)	Co(1)–C(12)–C(12')	77.8(5)		
C(1)–P–C(8)	104.0(7)	Co(2)–C(12)–C(12')	77.7(4)		
C(1)–P–C(8)	105.4(6)	Co(3)–C(12)–C(12')	77.2(6)		
Co(1)–P–C(8)	111.5(4)	Co(1)–C(12)–Co(2)	81.3(4)		
Co(1)–P–C(8)	116.5(5)	Co(2)–C(12)–Co(3)	80.9(4)		
Co(1)–P–C(8)	116.3(4)	Co(3)–Cl(2)L–Co(1)	80.0(4)		

2.2. A few aspects of NMR spectroscopy

Since the constitution of the complexes **5–7** follows unequivocally from elemental analysis, IR spectroscopy and X-ray diffraction, the application of NMR spectroscopy will only be discussed in the context of dynamic processes. ^{1}H, ^{13}C and ^{31}P NMR data are listed in Section 3. The ^{1}H NMR spectrum of **6** indicates free rotation about the sandwich- and C_{arene}–P-axes in that the *ortho-* and *meta-*arene protons are pairwise equivalent and a single signal is observed for the methyl protons of the PMe$_2$ groups. For the complex **7**, which is endowed with chelating coordination, the situation is less straightforward. The most conspicuous feature is selective broadening of the proton resonance lines in the η^6-arene region (Fig. 4). Since the sample shows a weak EPR signal, this broadening can be traced to electron self-exchange $7 + 7^+ \cdot \rightleftarrows 7^+ \cdot + 7$, the extent of broadening being proportional to the magnitude of the hyperfine coupling constant $a(^1H)$ [15c]. The usual procedure for destroying the paramagnetic exchange partner tempering the NMR sample fails in the present case because for **5–7** at $T > 40°$ decomposition sets in. Therefore, no information concerning structural flexibility of **7** can be extracted from the ^{1}H NMR spectrum in the (η^6-arene)proton region. However, two sharp doublets, split by the ^{31}P nucleus, are observed for the PMe$_2$ protons. This is indicative of fast interconversion (Scheme 2), because the sets of axial and equatorial methylprotons in **7** are diastereotopic giving rise to four signals in the slow and two signals in the fast exchange domain. Additional signals in the ^{1}H NMR spectrum of **7** are possibly caused by the presence of an isomer of **7** in which the equatorial rather than the axial positions at the CCo$_3$ cluster are spanned by the ligand **2**.

2.3. Electrochemistry and EPR

Cyclic voltammetry and EPR spectroscopy are strongly interrelated in the sense that the former may serve as a tool to probe whether radicals of sufficient lifetime for the application of the latter are accessible.

Table 2
Selected interatomic distances (pm) and bond angles (°) for **7**

Cr(1)–C(1)	217.0(7)	C(5)–C(6)	141.8(10)	Co(2)–C(10)	194.8(7)
Cr(1)–C(2)	215.8(7)	C(6)–C(1)	143.6(9)	Co(2)–C(13)	192.9(7)
Cr(1)–C(3)	214.6(7)	C(1)–P	181.7(7)	Co(2)–C(14)	174.6(8)
Cr(1)–C(4)	215.2(7)	C(7)–P	182.4(8)	Co(3)–C(11)	200.7(8)
Cr(1)–C(5)	213.9(7)	C(8)–P	182.7(7)	Co(3)–C(13)	203.5(8)
Cr(1)–C(6)	214.5(7)	C(1′)–P′	181.4(7)	Co(3)–C(15)	181.2(9)
Cr(1)–C(1′)	213.8(6)	C(7′)–P′	184.0(6)	Co(3)–C(16)	176.2(8)
Cr(1)–C(2′)	212.9(6)	C(8′)–P′	182.3(5)	C(9)–O(9)	112.6(8)
Cr(1)–C(3′)	214.1(7)	P–Co(1)	230.7(2)	C(10)–O(10)	117.3(8)
Cr(1)–C(4′)	215.3(7)	P′–Co(2)	225.5(2)	C(11)–O(11)	115.0(9)
Cr(1)–C(5′)	216.2(7)	Co(1)–Co(2)	249.0(2)	C(13)–O(13)	114.5(8)
Cr(1)–C(6′)	213.8(5)	Co(2)–Co(3)	250.1(1)	C(14)–O(14)	115.0(8)
C(1)–C(2)	139.9(10)	Co(3)–Co(1)	245.9(1)	C(15)–O(15)	113.7(8)
C(2)–C(3)	139.6(10)	Co(1)–C(9)	177.3(8)	C(16)–O(16)	114.7(8)
C(3)–C(4)	142.6(10)	Co(1)–C(10)	195.3(8)	C(12)–C(12′)	148.4(9)
C(4)–C(5)	138.2(11)	Co(1)–C(11)	188.5(9)		
C(6)–C(1)–C(2)	116.3(7)	C(1)–P–C(7)	103.4(4)		
C(1)–C(2)–C(3)	123.3(7)	C(1)–P–C(8)	98.3(3)		
C(2)–C(3)–C(4)	119.3(7)	C(1′)–P–C(7′)	102.0(3)		
C(3)–C(4)–C(5)	118.6(7)	C(1′)–P–C(8′)	105.3(3)		
C(4)–C(5)–C(6)	121.5(7)	P–Co(1)–Co(2)	118.4(7)		
C(5)–C(6)–C(1)	120.6(7)	P′–Co(2)–Co(1)	121.4(6)		
C(6′)–C(1′)–C(2′)	118.3(6)	C(1)–P–Co(1)	125.7(2)		
C(1′)–C(2′)–C(3′)	120.5(7)	C(1′)–P′–Co(2)	118.0(2)		
C(2′)–C(3′)–C(4′)	120.1(7)	C(8)–P–Co(1)	109.8(12)		
C(3′)–C(4′)–C(5′)	119.5(7)	C(7)–P–Co(1)	114.4(3)		
C(4′)–C(5′)–C(6′)	120.9(7)	C(7′)–P–Co(2)	112.7(2)		
C(5′)–C(6′)–C(1′)	120.8(6)	C(8′)–P–Co(2)	116.1(2)		
C(7)–P–C(8)	101.6(4)	Co(1)–CO(2)–Co(3)	59.0(5)		
C(7′)–P–C(8′)	100.2(3)	Co(3)–Co(1)–Co(2)	60.2(4)		
Co(2)–Co(3)–Co(1)	60.2(4)	Co(1)–C(12)–Co(12′)	130.9(5)		
Co(2)–C(10)–Co(1)	79.3(3)	Co(2)–C(12)–Co(12′)	133.2(6)		
Co(1)–C(11)–Co(3)	78.3(3)	Co(3)–C(12)–Co(12′)	130.7(5)		
Co(3)–C(13)–Co(2)	78.3(3)	Co(1)–C(12)–Co(3)	79.2(3)		
P–Co(1)–C(9)	98.9(2)	Co(1)–C(12)–Co(2)	81.1(3)		
C(15)–Co(3)–C(16)	102.9(3)	Co(2)–C(12)–Co(3)	81.6(3)		
P′–Co(2)–C(14)	95.3(3)				

OC
OC
Mn
P'''Me
Me

Me
P'''Me
Cr

Me
Me
P
Mn
''''CO
CO
8

(CO)₃
Co
(CO)₃Co
Co
(CO)₂
P
Ph₂
C
Me

Me
C
P—eq—Co
Ph₂
Co—Co(CO)₃
C CO (CO)₃
O
Fe
9

Ph₂
P ax
(CO)₂
Fe
Co
(CO)₃
Co
CMe(Ph)
Co
P
(CO)₂
Ph₂
10

Fo2

Mull
(Nujol)

Solution
(Toluene)

7

2200 2100 2000 1900 1800 1700 cm⁻¹   2200 2000 1900 1800 1700 1600 cm⁻¹

6

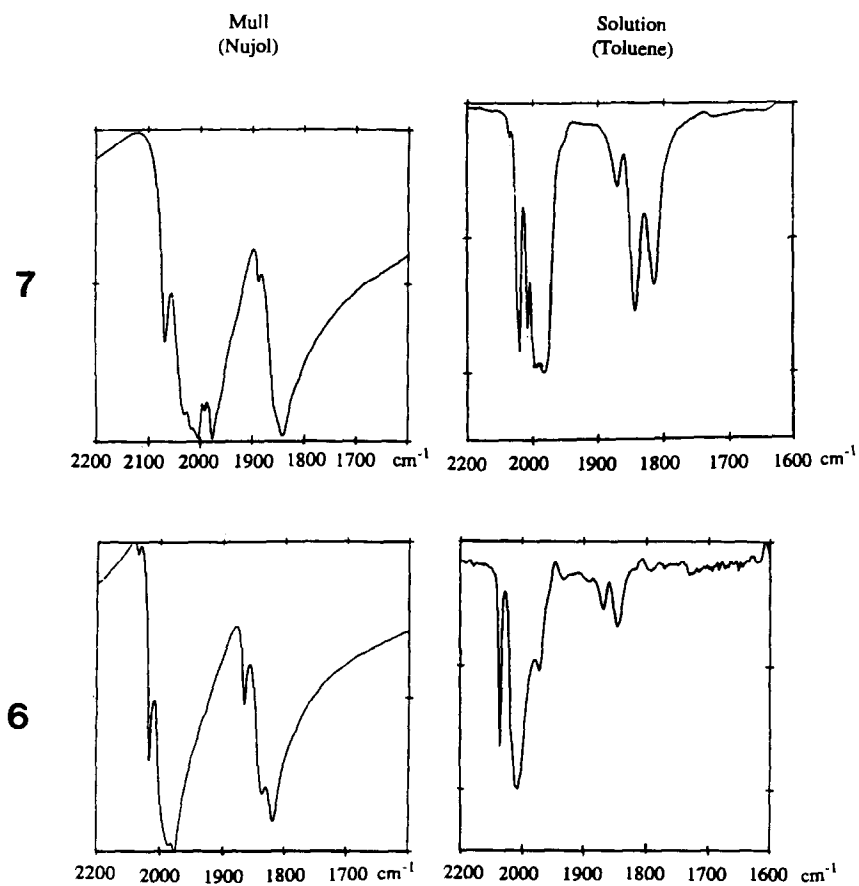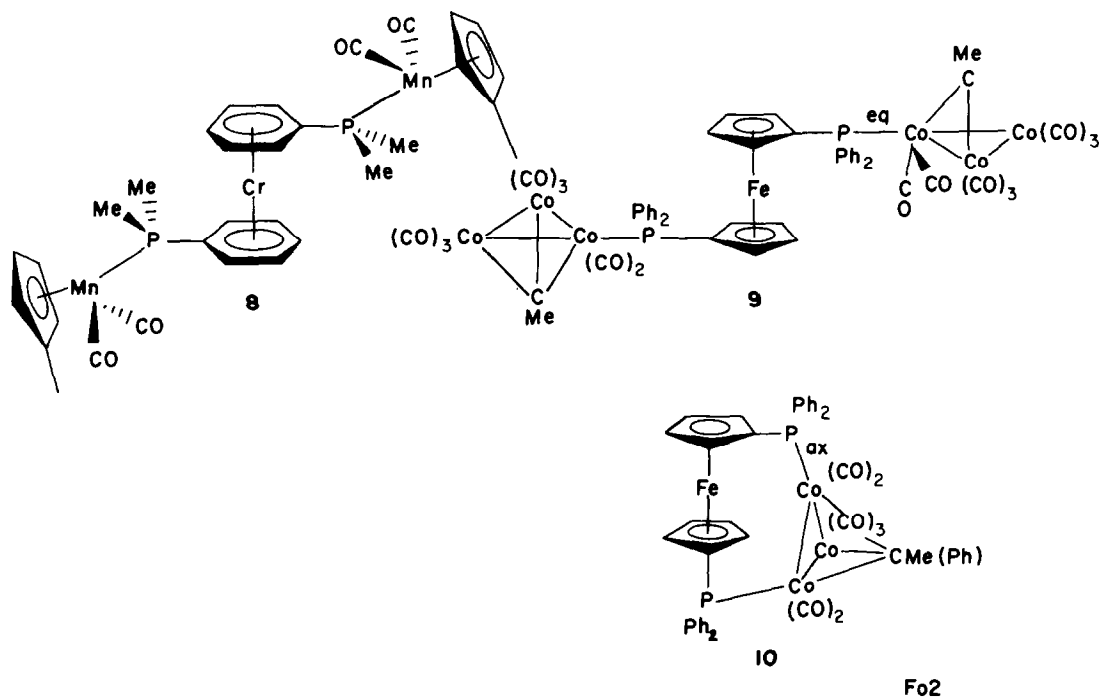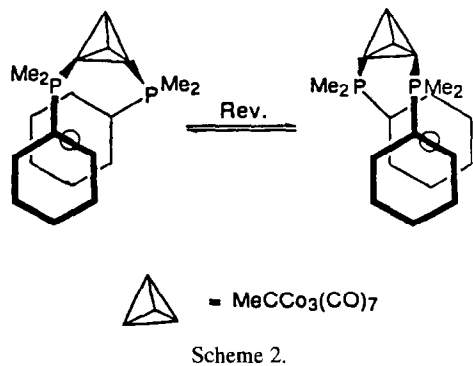2200 2000 1900 1800 1700 cm⁻¹   2200 2000 1900 1800 1700 1600 cm⁻¹

Fig. 3. IR spectra (carbonyl range) of compounds 6 and 7 recorded in solution (toluene) and from a mull (nujol).

Scheme 2.

The electrochemical reduction of **3** and its phosphane substituted derivatives has been the subject of several studies, culminating in a comprehensive report by Heinze et al. [4a]. The situation is complicated by the fact that the initially generated 49 VE radical anions of phosphane-substituted clusters tend to eliminate R_3P or CO to yield 47 VE monoanions that can either react with liberated phosphine or CO or, in a second electron-transfer step, form dianions. The complexes **5–7** contain two redox centers — the μ-CCo_3 cluster and the bis(arene)chromium units — posing the ques-
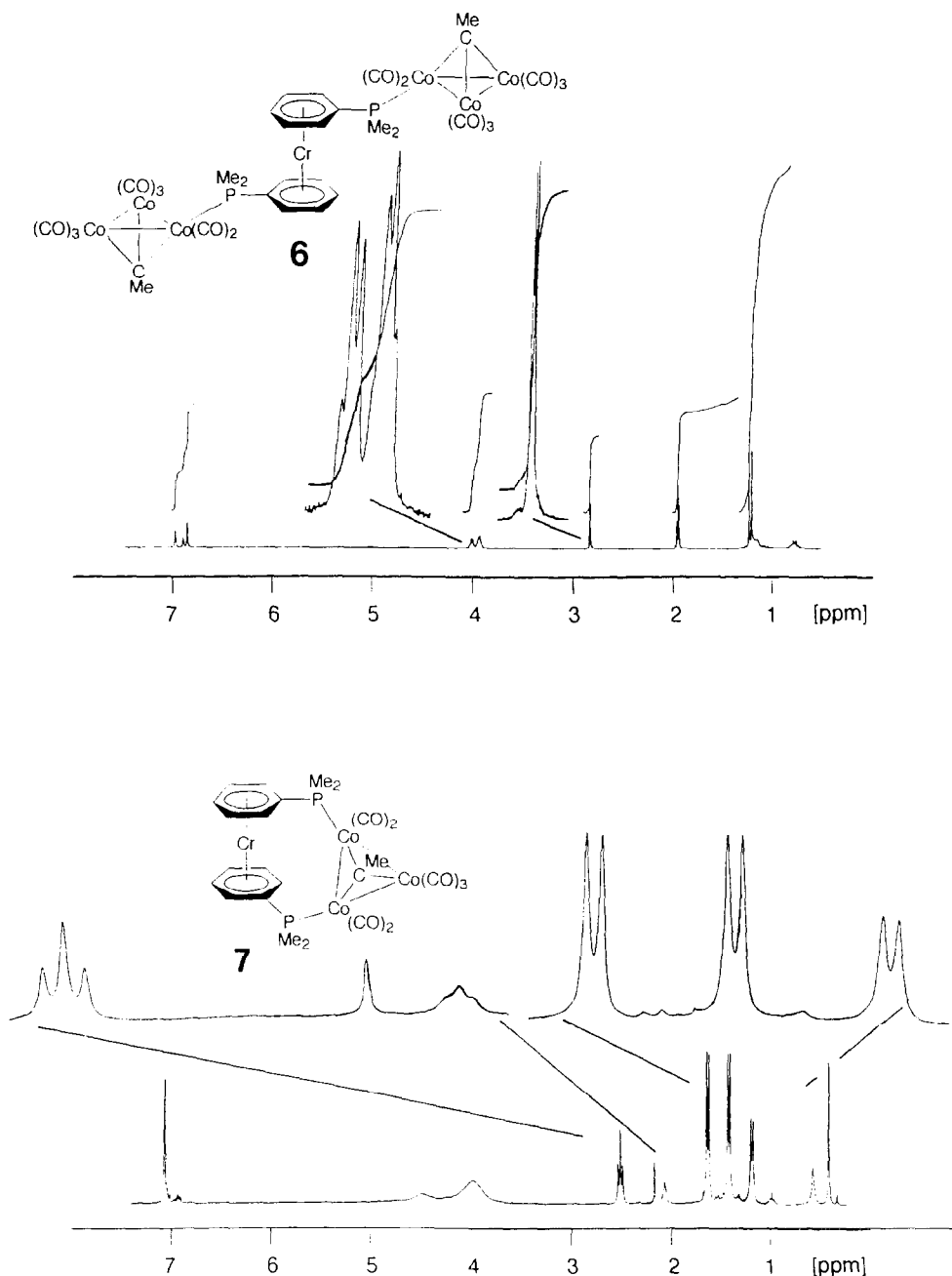

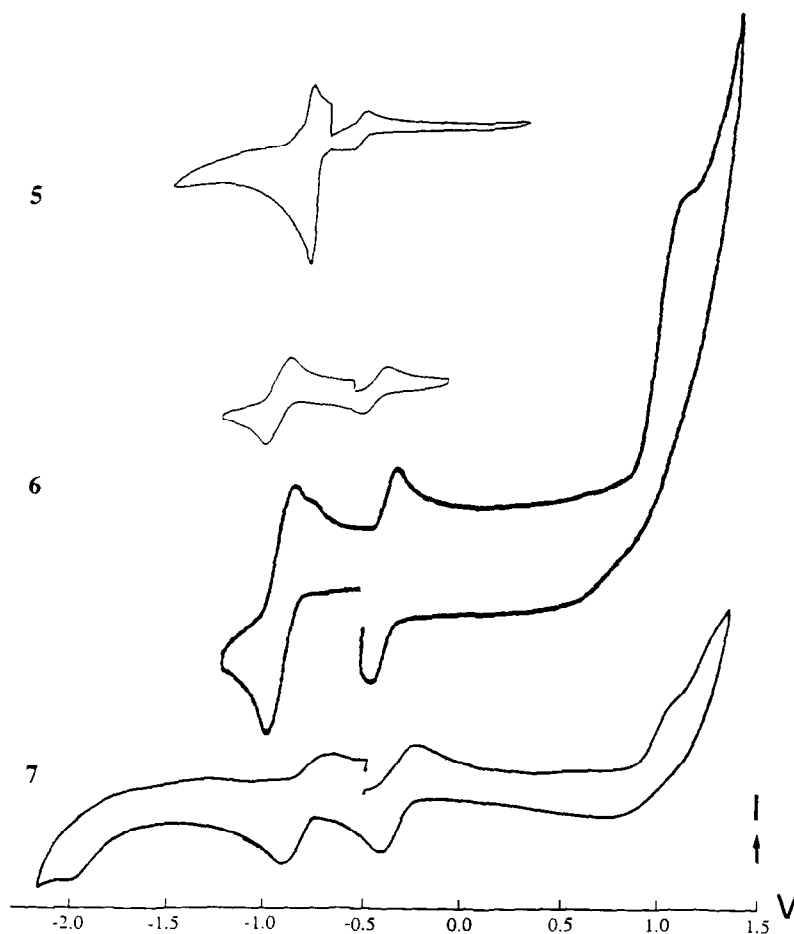Fig. 4. ^{1}H NMR spectra of **6** and **7**.

Fig. 5. Cyclovoltammetric traces for the complexes 5-7 in dimethoxyethane (0.1 M Bu_4NClO_4) at glassy carbon vs. SCE.

tion as to their mutual interaction. Cyclovoltammetric traces for the compounds 5-7 are shown in Fig. 5 and the respective electrochemical data are collected in Table 3. In all three cases, the redox couple $Cr^{+/0}$ is reversible; compared with the parent bis(η^6-benzene)-chromium ($E_{1/2}^{+/0} = -0.72$ V at $-35°C$ [17]) replace-

Table 3
Cyclovoltammetric data of the complexes 5, 6 and 7 (in dimethoxy ethane containing 0.1 M Bu_4NClO_4 at glassy carbon vs. SCE, $v = 100$ mV s^{-1})

	T (°C)	$E_{1/2}$ (0/ + 1) (V)	ΔE_p (mV)	i_{pa}/i_{pc}	n [a]	$E_{1/2}$(0/ − 1,− 2) (V)	ΔE_p (mV)	i_{pa}/i_{pc}	n [a]	E_{pa} [b] (V)	E_{pc} [b] (V)
mdme	25	−0.62 [c] Cr^0-Cr^1	65	1.00	1					1.28	
bdme	25	−0.57 [c] Cr^0-Cr^1	63	1.00	1					1.42	
$MeCCo_3(CO)_9$ 5	25	1.30 [b] Co			1	−0.55 [c]	94	1.01	1		−1.718
$MeCCo_3(CO)_8$ (mdme) 6	−40	−0.51 [c] Cr^0-Cr^1	76	1.01	1	−0.75 [b] Co			1	0.85	
$MeCCo_3(CO)_7$ (bdme) 7	−55	−0.44 [c] Cr^0-Cr^1	110	0.95	1	−0.93 [c] Co	250	0.84	1	0.55	−2.05
$[MeCCo_3(CO)_8]_2$ (μ-bdme)	−68	−0.39 [c] Cr^0-Cr^1	120	1.00	1	−0.91 [c] Co	110	1.10	2	0.65	−1.94

[a] Number of electrons transferred.
[b] Irreversible.
[c] Reversible.

ment of ring protons by (μ-MeC)Co$_3$(CO)$_{9-n}$(Me$_2$P-)$_n$ ($n = 1$ or 2) units effects anodic shifts which, in accord with the presence of several electron withdrawing CO ligands, are particularly large. The simplest reduction behavior is exhibited by the interannularly bridged complex **7**: in addition to the redox couple of the sandwich unit a quasireversible wave caused by cluster reduction is observed. From a comparison with the peak current of the couple **7**$^{+/0}$, which may serve as an internal reference, single electron transfer is inferred for the reduction of **7**. Compared with the couple **3**$^{0/-}$ of the parent cluster (μ-MeC)Co$_3$(CO)$_9$, the potential for **7**$^{0/-}$ is shifted cathodically because, upon substitution of CO by phosphanes, the intra-cluster electron density is increased. The magnitude of the shift ($\delta E_{1/2} = -0.38$ V) caused by the substitution of two CO ligands is in qualitative agreement with the substituent parameter $\delta E_{1/2}$(PPh$_3$) $= -0.23$ V given previously [4b].

Whereas the peak separation and its dependence on scan rate point at electrochemical quasi-reversibility, the peak-current ratio suggests that the couple **7**$^{0/-}$ is chemically reversible. Thus, the frequently encountered loss of a phosphane ligand L following electron transfer to a cluster (μ-RC)Co$_3$(CO)$_8$L is suppressed if chelating coordination of the type (μ-RC)Co$_3$(CO)$_7$(L-L) prevails. Nevertheless, the complex **6** which contains two Me$_2$P-coordinated (μ-MeC)Co$_3$(CO)$_8$ units display similar electrochemical behavior as **7** albeit with a peak-current ratio of 1:2 for the processes **6**$^{+/0}$ and **6**$^{0/-2}$, respectively. By this, we do not want to imply that reduction represents a two-electron transfer but, rather, that the interaction between the two terminal clusters, separated by the bifunctional sandwich complex **2**, is too small to lead to a resolved redox splitting in the cyclovoltammetric trace. The shape of the CV trace for the monosubstituted derivative **5** is unusual and somewhat reminiscent of the CV behavior of (μ-MeC)Co$_2$CO$_6$(PEt$_2$Ph)$_3$ [18].

Since the diamagnetic oligonuclear complexes **5–7** proved to be susceptible to one-electron oxidation and reduction, an investigation of these processes by means of EPR spectroscopy was performed. Upon oxidation by air or 4-pyridinecarbaldehyde, **5–7** readily yield radical cations which give rise to the EPR spectra shown in Fig. 6. The respective data are listed in the caption. Radical stability decreases according to **7**$^+\cdot$ > **5**$^+\cdot$ $\gg$ **6**$^+\cdot$. Therefore, resolved spectra of **6**$^+\cdot$ could not be obtained, the half-life of this species being only a few minutes. While **7**$^+\cdot$ and **6**$^+\cdot$ show indications of ^{1}H and ^{31}P hyperfine splittings, insufficient resolution precludes complete analysis and simulation. However, the gradation $a(^1$H, **5**$^+\cdot$) > $a(^1$H, **7**$^+\cdot$) is real and reflects the stronger electron withdrawing effect that the Co$_3$C-cluster excerts if connected to the bis(arene)metal unit by two (**7**$^+\cdot$) rather than one (**5**$^+\cdot$)-PMe$_2$-links.
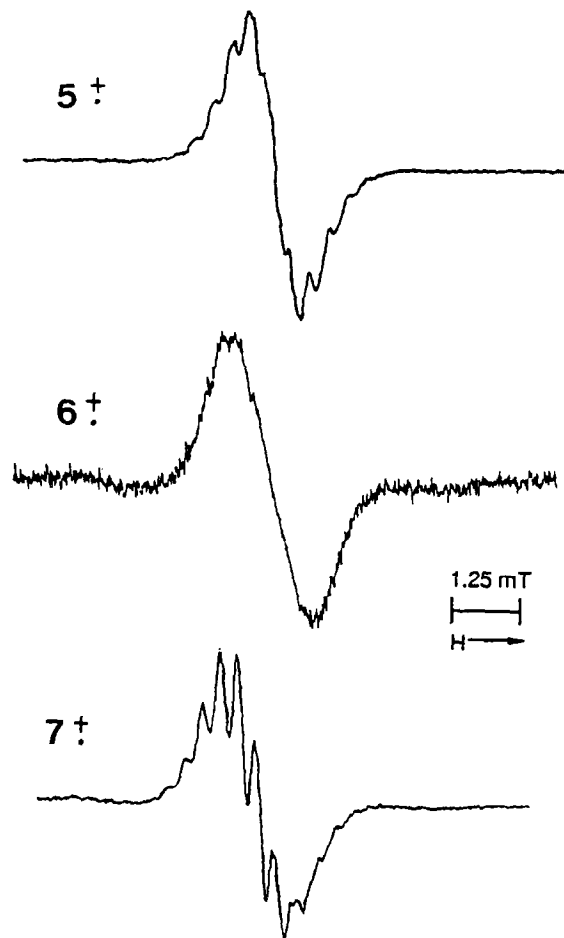
Reduction of phosphane-substituted clusters (μ-

Fig. 6. EPR spectra (X-band, THF, 20°C) of the radical cations **5**$^+\cdot$, **6**$^+\cdot$ and **7**$^+\cdot$ generated by oxidation of the diamagnetic precursors with 4-pyridine carbaldehyde. **5**$^+\cdot$: $\langle g \rangle = 1.9842$, $a(^1$H) $= 0.333$ mT, $a(^{31}$P) ≈ 0.12 mT; **6**$^+\cdot$: $\langle g \rangle = 1.9843$; **7**$^+\cdot$: $\langle g \rangle = 1.9872$, $a(^1$H) $= 0.316$ mT.

RC)Co$_3$(CO)$_{9-n}$L$_n$ has in the past led to EPR-silent solutions [4b] or to the EPR spectrum of the parent cluster radical anion (μ-RC)Co$_3$(CO)$_9^-$, [19], the latter being formed via elimination of a phosphane ligand and incorporation of CO present in solution. Identical behavior is exhibited by the complexes **5** and **6** which upon electrochemical reduction in the EPR cavity as well as via reduction with alkali metals yielded an EPR spectrum of **3**$^-\cdot$ [20]. In the case of the chelate complex **7**, in situ reduction, even if carried out at −40°C, failed to yield an EPR signal. Reduction of the bis-phosphane-substituted species possibly leads to cluster degradation rather than to substitution of phosphane by CO.

2.4. Establishing the ETC mechanism for the formation of 5–7

As mentioned above, the synthesis of **5–7** from **3** and **1** or **2** proceeds readily at room temperature without
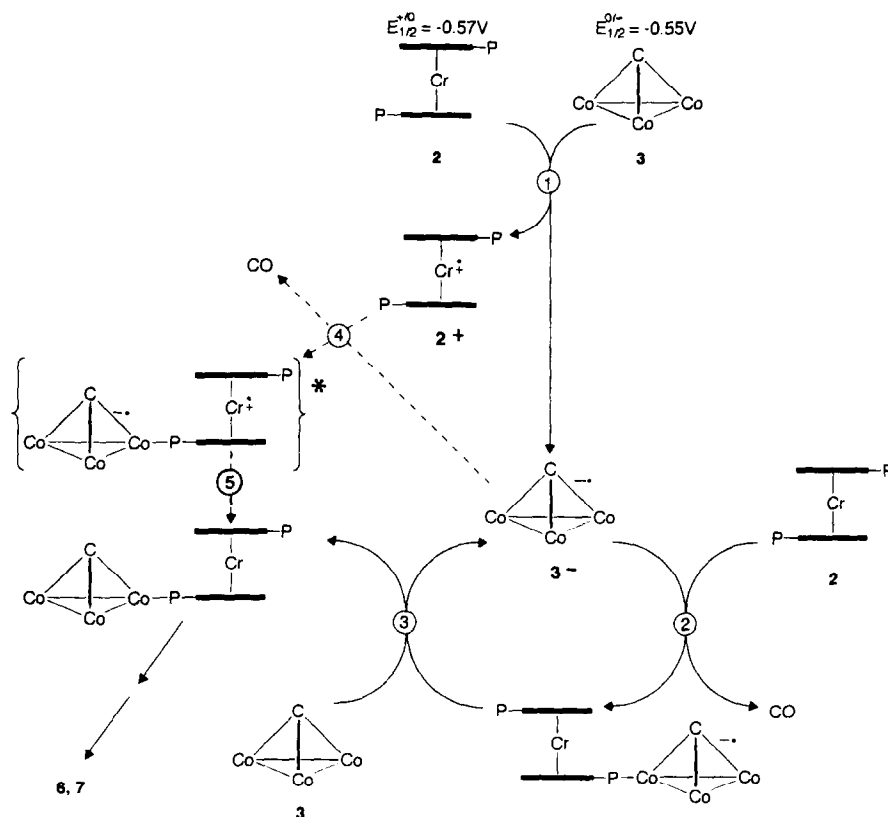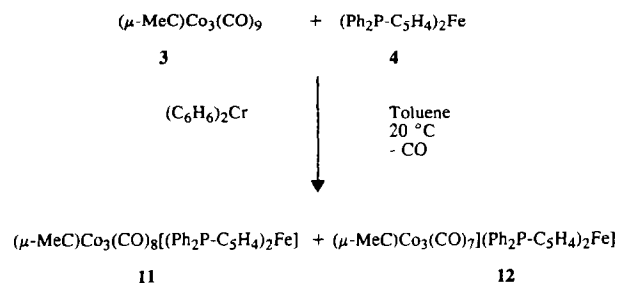
Scheme 3.

irradiation or initiation through addition of a redox catalyst. This behavior, which contrasts with that of the related ferrocene based ligand 4, can be traced to the differing redox potentials for the couples $(\eta^5 - C_5H_5)_2Fe^{+/0}$ $(E_{1/2} = +0.49$ V) and $(\eta^6 - C_6H_6)_2Cr^{+/0}(E_{1/2} = -0.69$ V at 25°C). Thus, a catalysis chain will be triggered by electron transfer between the educts 3 and 1 or 2, respectively, with initial formation of 3$^-$· which is much more prone to substitution than neutral 3 [21]. The steps leading to the products are presented in Scheme 3. The cycle is initiated by step (1) which, according to the redox potentials $E_{1/2}(2^{+/0})$ and $E_{1/2}(3^{0/-})$, generates equilibrium concentrations of 2$^+$· and 3$^-$·. The cluster anion 3$^-$· is substituted by 2 in step (2), and in step (3) the product anion is reoxidized by neutral 3 forming 3$^-$· which continues the chain. Step (3) is thermodynamically favorable since phosphane substitution at carbonyl clusters effects an anodic shift of the redox potential thereby destabilizing the substituted relative to the parent cluster anion. In a parallel minor path (4), 3$^-$ may also react with 2$^+$ to yield a substituted cluster zwitterion which immediately relaxes by intramolecular ET to the neutral product (step (5)). As judged from the redox potentials of the constituting moieties, the zwitterion represents an electronically excited state. Repetition of the steps described above will lead to the products 6 and 7. Interest-

ingly, the reaction between the ferrocene analog $(Ph_2P - C_5H_4)_2Fe$ (4) and the cluster 3, which fails to proceed at room temperature, may be initiated by the addition of a small amount of bis(benzene)chromium 10, thereby supporting the ETC mechanism suggested for the reaction of 2.

There is also EPR evidence for the initiating step (1): if solutions of bis(benzene)chromium 10 and (μ-MeC)Co$_3$(CO)$_9$ 3 are combined, a spectrum is observed which is the result of the superposition of the spectra of 10$^+$· and 3$^-$· (Fig. 7). The activation of diamagnetic metal carbonyls for ligand substitution by electron transfer is, of course, well established [4c,24] and to this end, electron-rich sandwich complexes have been used previously. Examples are the reaction between binuclear (μ-fulvalene)metal carbonyl complexes and PR$_3$, initi-

$(\mu\text{-MeC})Co_3(CO)_9$ + $(Ph_2P\text{-}C_5H_4)_2Fe$

3   **4**

$(C_6H_6)_2Cr$ Toluene
                           20 °C
                           - CO

$(\mu\text{-MeC})Co_3(CO)_8[(Ph_2P\text{-}C_5H_4)_2Fe]$ + $(\mu\text{-MeC})Co_3(CO)_7[(Ph_2P\text{-}C_5H_4)_2Fe]$

11   **12**

Scheme 4.

ated by $(C_5H_5)Fe(C_6R_6)$ [25], and that of $BrMn(CO)_5$ with $Ph_2P(CH_2)_2PPh_2$ which is started by catalytic amounts of **10** [26]. A particularly interesting aspect of the formation mechanism of **5–7**, as detailed in Scheme 3, is the fact that **1** and **2** simultaneously act as initiators and as ligands. The mechanism therefore constitutes an electron transfer chain autocatalysis where the ligands **1** and **2** play the role of electron donor and the metal carbonyl cluster **3** that of electron acceptor. An ETC autocatalysis with an inverse direction of initial electron flow has been described previously: the reaction between $(Me_5C_5)Mn(CO)_2(THF)$ and tetracyanoethene (TCNE) is triggered by an electron transfer from the halfsandwich complex to the ligand TCNE, thereby generating the substitution labile 17 VE species $(Me_5C_5)Mn(CO)_2(THF)^+ \cdot$ [27].
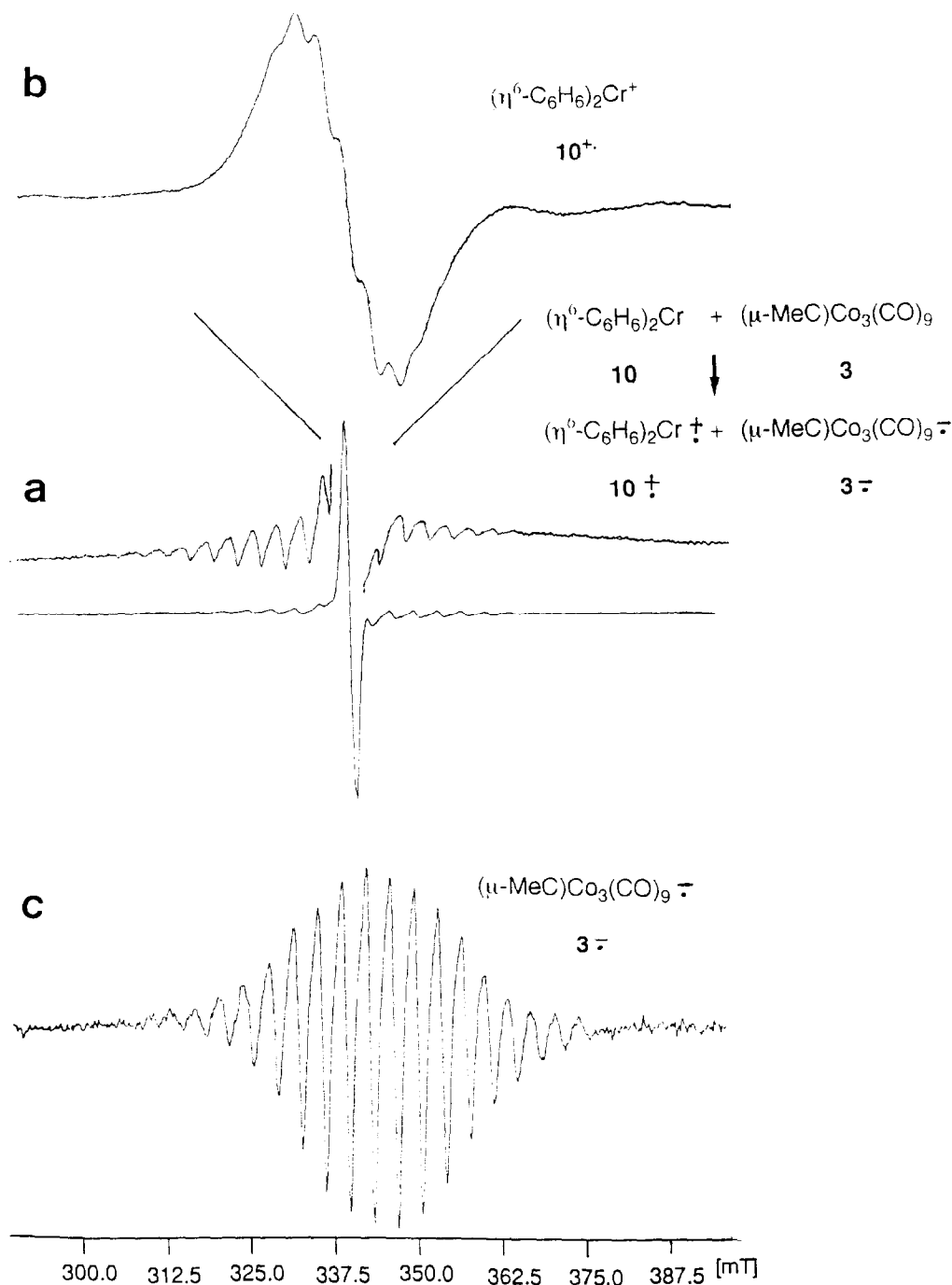

Fig. 7. (a) EPR spectrum (X-band, THF, 20°C) obtained upon combining solutions of the diamagnetic precursors **3** and **10**; (b) EPR of **10⁺·** in THF, expanded scale; (c) EPR of **3⁻·**, original scale.

3. Experimental details

All manipulations were carried out with exclusion of air under dinitrogen or argon (CV). Physical measurements were performed with the equipment specified previously [22].

3.1. [(Dimethylphosphano-η^6-benzene)(η^6-benzene)chromium](octacarbonyl)-(μ_3-ethylidyne)-triangulo-tricobalt(3Co–Co) (5)

To a solution of (dimethylphosphano-η^6-benzene)(η^6-benzene)chromium (1) [5] (0.52 g, 1.4 mmol) in 50 ml of toluene was added within 1 h at 25°C a solution of (nonacarbonyl)-(μ_3-ethylidyne)-triangulo-tricobalt(3Co–Co) (3) [23] (1.14 g, 2.5 mmol) in 30 ml of toluene. Effervescence sets in immediately. Stirring at room temperature was continued for 5 h whereupon the color changes from brown to dark violet. After removing the solvent at high vacuum the residue was subjected to column chromatography (stationary phase Al_2O_3, 3% H_2O: mobile phase toluene; dimensions 3 × 20 cm). The first band to be eluted contained unreacted 3 (0.38 g, 0.83 mmol) the second band consisted of the product 5 which was obtained as a dark violet oil which resisted solidification. Yield of 5: 0.32 g (0.46 mmol). The product 3 is very soluble in petroleum ether, toluene and THF rendering attempts at crystallization unsuccessful. Anal. Found: C, 40.88; H, 2.28%. $C_{24}H_{20}CrCo_3O_8P$ Calc.: C, 41.41; H, 2.29%. No ^1H or ^{13}C NMR data available owing to self-exchange induced line broadening. ^{31}P NMR (C_6D_6, room temperature): δ 23.4, $\Delta\delta$ ^{31}P (5–1) 65.7.

3.2. μ-[Bis(dimethylphosphano-η^6-benzene)chromium]bis[(octacarbonyl)-(μ_3-ethylidyne)-triangulo-tricobalt(3Co–Co)] (6)

To a mixture of bis(dimethylphosphano-η^6-benzene)chromium (2) [5] (0.50 g, 1.71 mmol) and (μ-MeC)Co$_3$(CO)$_9$ (3) (1.60 g, 3.51 mmol) 30 ml of toluene were added at 25°C. The dissolution was accompanied by vigorous effervescence and the color change from violet to dark brown. After stirring for 8 h the solvent was removed at high vacuum. The residue, a dark brown oil, was washed with two 10 ml portions of petroleum ether 40/60 and chromatographed (Al_2O_3, 3% H_2O; toluene). A weak pink band was followed by dark violet and brown bands, the latter two not separating completely. From band 1, 15 mg (1%) of 3 were isolated; Band 3 contained 40 mg (3%) of the chelate complex 7. Complexes 3 and 7 were characterized by means of IR spectroscopy. The residue from band 2 was recrystallized from hexane (30 ml) to yield 0.28 g (14%) of 6 as dark violet crystals. Anal. Found: C, 36.21; H, 2.38%. $C_{36}H_{28}CrCo_6O_{16}P_2$ Calc.: C, 36.52;

H, 2.38%. ^1H NMR (C_6D_6, room temperature): δ 4.00 (m, H2, 4, 6), δ 4.08 (t, H3, 5), δ 1.30 (d, H7, 8, ^2J(H7,8–P) = 8.8 Hz)), δ 1.8 (d,H9, ^5J(H9–P) = 1.8 Hz)). ^{13}C NMR ($C_6D_5CD_3$, $-$ 40°C): δ 89.4 (C1, ^1J(C1,P) = 44.3 Hz), δ 75.3 (C2, 6, ^2J(C2,P) = 12.5 Hz)), δ 75.7 (C3, 5, ^3J(C3,P) = 6.7 Hz)), δ 74.5 (C4), δ 15.3 (C7, 8), δ 42.3 (C9), δ 208.2 (CO). ^{31}P NMR (C_6D_6, room temperature): δ 23.5, $\Delta\delta$ ^{31}P (6–2) 66.1. IR (Nujol): ν(CO) 2067 (46.3), 2040 (55.1), 2015 (62.1), 1995 (52.1), 1977 (64.2), 1880 (35.2), 1842 (63.5) cm^{-1}. IR (toluene): ν(CO) 2070 (83.1), 2014 (100), 1932 (53.9), 1868 (30.2), 1846 (36.5) cm^{-1}.

3.3. [Bis(dimethylphosphano-η^6-benzene)chromium](heptacarbonyl)-(μ_3-ethylidyne)-triangulo-tricobalt (3Co–Co) (7)

To a solution of 2 (0.57 g, 1.73 mmol) in 500 ml of toluene was added a solution of 3 (0.62 g, 1.73 mmol) in 250 ml of toluene during 3 h at room temperature. Stirring was continued for 12 h and completeness of reaction was followed by IR spectroscopy. The solvent was distilled off and the residue was chromatographed at $Al_2O_3/1\%$ (3 × 41 cm, elution with toluene). A narrow dark violet band was followed by a broad reddish-brown band. According to IR identification, the first band contained the complex 6 (30 mg, 1%); the second eluate was reduced in volume to 10 ml and layered with 30 ml of n-hexane. At $-$ 20°C, 7 (0.32 g 25%) was obtained as small reddish-brown prisms. Anal. Found: C, 46.99; H, 3.32%. $C_{25}H_{25}CrCo_3O_7P_2$ Calc.: C, 41.23; H, 3.45%. ^1H NMR (C_6D_6, room temperature): δ 3.97 (self-exchange broadened), δ 4.49 (self-exchange broadened), δ 1.33 (d, H7, ^2J(H7, P) = 7.2 Hz)), δ 1.55 (d, H8, ^2J(H8, P) = 7.2 Hz)), δ 2.45 (t, H9, ^5J(H9, P) = 7.1 Hz)). ^{13}C NMR (C_6D_6, room temperature): δ 86.8 (C1, ^1J(C1, P) = 28.4 Hz)), δ 79.0 (C2, ^2J(C2, P) = 12.8 Hz)), δ 76.6 (C3), δ 75.2 (C4), δ 74.9 (C5), δ 77.5 (C6), δ 19.5 (C7), δ 17.4, (C8), δ 40.6 (C9), δ 218.5 (CO). ^{31}P NMR (C_6D_6, room temperature) δ 8.1, $\Delta\delta$ ^{31}P (7–2) 50.7. IR (Nujol): ν(CO) 2030 (61.8), 1984 (82.0), 1976 (85.9), 1865 (47.3), 1835 /70.9), 1818 (78.0) cm^{-1}. IR (toluene): ν(CO) 2039 (91.6), 2013 (83.6), 1994 (97.7), 1981 (100), 1869 (31.2), 1843 (77.6), 1814 (68.5) cm^{-1}.

3.4. Synthesis of [bis(diphenylphosphano-η^5-cyclopentadienyl)iron](heptacarbonyl)-(μ_3-ethylidyne)-triangulo-tricobalt(3Co–Co) (12) employing bis(benzene)chromium (10) as an ET-catalyst

Bis(diphenylphosphano-η^5-cyclopentadienyl)iron (4) (0.29 g, 0.52 mmol) and (μ-MeC)Co$_3$(CO)$_9$ (3) (0.32 g, 0.53 mol) were dissolved in 40 ml of toluene. No evolution of gas was observed. After the addition of a solution of bis(benzene)chromium (10) (10.8 mg, 0.052

mmol) in 15 ml of toluene effervescence set in. The solution was stirred for 200 min, the volume of gas evolved being monitored (reaction time (min)/CO (ml): 10/6.5, 20/10.5, 30/13.5, 40/14.75, 50/16.25, 60/16.75, 70/18.5, 80/19.0, 120/21.5, 200/22.0, i.e. 94% for the release of 2 CO/3). The solution was concentrated to 5 ml and chromatographed (Al$_2$O$_3$/1% H$_2$O, 3 × 15 cm, elution with toluene). A very weak greenish band of 10 was followed by a broad red violet band. The residue of the latter was recrystallized from toluene/petroleum ether (1:4) to yield 12 (0.27 g, 51%), identified by means of ^{1}H, ^{13}C, ^{31}P NMR and IR spectroscopies [6].

3.5. X-Ray structure determination of compounds 6 and 7

Crystal data and other parameters related to the structure determination are listed in Table 4. Atomic coordinates and equivalent isotropic displacement parameters are collected in Tables 5 and 6, while the most significant bond lengths and angles are given in Tables 1 and 2 [28].

3.5.1. Data collection and reduction for 6

The crystal (0.3 × 0.25 × 0.2 mm^3) was mounted in inert oil on a glass fibre which was placed in the cold gas stream of the diffractometer (Siemens R3m/V with LT-2 low temperature attachment). Data were collected to $2\theta = 52°$ with monochromated Mo Kα radiation. Cell constants were refined from diffractometer angles of 31 reflections with $2\theta > 15°$. Of 4881 reflections, 4062 were unique ($R_{int} = 0.0763$).

3.5.2. Structure solution and refinement for 6

The structure was solved by direct methods. Nonhydrogen atoms were refined anisotropically, hydrogens were included using a riding model with fixed isotropic temperature factors. Refinement on F (program SHELX-76) proceeded to $R = 0.0782$, $wR = 0.0743$ for 2419 reflections with $F > 4\sigma(F)$. The weighting scheme was

Table 4
Crystallographic data for 6 and 7

	6	7
Empirical formula	C$_{36}$H$_{28}$Co$_6$CrO$_{16}$P$_2$	C$_{25}$H$_{25}$Co$_3$CrO$_7$P$_2$
Formula weight	1184.1	728.18
Temperature (K)	203(2)	223(2) K
Wavelength (Å)	0.71073	0.71073
Crystal system	Triclinic	Triclinic
Space group	P$\bar{1}$	P$\bar{1}$
Unit cell dimensions		
a (Å)	8.625(4)	10.474(2)
b (Å)	10.057(5)	10.6800(10)
c (Å)	12.827(6)	14.424(2)
α (°)	106.54(3)	90.360(10)
β (°)	94.86(3)	110.340(10)
γ (°)	93.52(4)	113.320(10)
Volume (Å^3)	1058.5(9)	1369.8(3)
Z	1	2
Density calculated (Mg m^{-3})	1.858	1.766
Absorption coefficient (mm^{-1})	2.684	2.330
$F(000)$	588	732
Crystal size (mm)	0.3 × 0.25 × 0.2	0.3 × 0.2 × 0.2
θ range for data collection (°)	1–26	1.53–25.96
Index ranges	$-1 \le h \le 10$, $-11 \le k \le 11$, $-15 \le l \le 15$	$0 \le h \le 10$, $-11 \le k \le 10$, $-15 \le l \le 14$
Reflections collected	4881	3836
Independent reflections	4062 [$R_{int} = 0.0763$)	3509 [$R_{int} = 0.0283$]
Absorption correction	DIFABS	
Refinement method	Full-matrix least squares on F	Full-matrix least-squares on F^2
Data/restraints/parameters	2419 ($F > 4\sigma(F)$/0/277	3508/0/340
Goodness-of-fit on F^2		0.840
Goodness-of-fit on F	2.02	
Final R indices [I > 2σ(I)]	$R = 0.0782$, $wR = 0.0743$	$R = 0.0435$, $wR_2 = 0.0928$
R indices (all data)	$R = 0.1227$, $wR = 0.0792$	$R = 0.0732$, $wR_2 = 0.1139$
Weighting sheme	$w^{-1} = \sigma^2(F)$	$w^{-1} = \sigma^2(F_o^2) + (0.0495p)^2$ $p = (F_o^2 + 2F_c)^2/3$
Largest diff. peak and hole (e Å^{-3})	1.09 and -1.03	0.798 and -0.712

$w^{-1} = \sigma^2(F)$; max $\Delta\rho = 1.09$ e Å^{-3}. The data were corrected with the program DIFABS.

3.5.3. Data collection and reduction for 7

The crystal ($0.3 \times 0.2 \times 0.2$ mm^3) was mounted in inert oil on a glass fibre which was placed in the cold gas stream of the diffractometer (Siemens P4 with LT-2 low temperature attachment). Data were collected to $2\theta = 52°$ with monochromated Mo Kα radiation. Cell constants were refined from diffractometer angles of 32 reflections with $2\theta > 20°$. Of 3836 reflections, 3509 were unique ($R_{int} = 0.0283$).

3.5.4. Structure solution and refinement for 7

The structure was solved by direct methods. Nonhydrogen atoms were refined anisotropically, hydrogens were included using a riding model with fixed isotropic temperature factors. Refinement on F^2 (program SHELXL-93) proceeded to $wR2 = 0.0928$ for all data (conventional $R = 0.0435$ for 2241 reflections with $F > 4\sigma(F)$). The weighting scheme was $w^{-1} = \sigma^2(F_0^2)$

Table 5

Atomic coordinates and equivalent isotropic displacement parameters [Å^2] for 6. U_{eq} is defined as one third of the trace of the orthogonalized U_{ij} tensor

Atom	x	y	z	U_{eq}
Co(1)	0.3612(2)	0.2949(1)	0.7905(2)	0.020(1)
Co(2)	0.4338(2)	0.2636(2)	0.6056(2)	0.022(1)
Co(3)	0.3088(2)	0.4731(2)	0.6957(2)	0.023(1)
Cr	0	0	1	0.021(1)
P	0.1510(3)	0.1477(3)	0.7914(3)	0.021(1)
C(1)	0.5000(13)	0.4078(10)	0.7360(11)	0.021(4)
C(2)	0.6593(13)	0.4820(11)	0.7873(11)	0.028(5)
C(3)	0.4648(13)	0.1441(11)	0.6998(10)	0.020(4)
O(3)	0.5221(11)	0.0422(8)	0.7015(9)	0.043(4)
C(4)	0.3471(13)	0.4078(11)	0.5433(12)	0.023(5)
O(4)	0.3315(11)	0.4303(9)	0.4603(9)	0.038(4)
C(5)	0.2397(15)	0.4469(12)	0.8382(11)	0.027(5)
O(5)	0.1638(11)	0.5038(9)	0.034(8)	0.039(4)
C(11)	0.4700(14)	0.3020(11)	0.0023(13)	0.027(5)
O(11)	0.5395(12)	0.3040(10)	0.9933(9)	0.050(4)
C(21)	0.6161(15)	0.2545(12)	0.5497(12)	0.029(5)
O(21)	0.7326(11)	0.2487(9)	0.5162(9)	0.044(4)
C(22)	0.3029(13)	0.1354(12)	0.5050(12)	0.026(5)
O(22)	0.2171(11)	0.0582(10)	0.4433(8)	0.049(4)
C(31)	0.3897(13)	0.6484(13)	0.7370(12)	0.029(5)
O(31)	0.4446(11)	0.7598(8)	0.7632(10)	0.052(5)
C(32)	0.1066(14)	0.4883(11)	0.6544(11)	0.026(5)
O(32)	−0.0163(12)	0.5053(11)	0.6288(10)	0.058(5)
C(6)	0.1422(14)	−0.0274(11)	0.6969(12)	0.029(5)
C(7)	−0.0398(14)	0.2012(12)	0.7575(12)	0.036(5)
C(41)	0.1401(14)	0.1239(10)	0.9221(10)	0.022(4)
C(42)	0.2371(13)	0.0246(12)	0.9542(13)	0.033(5)
C(43)	0.2433(14)	0.0179(14)	1.0647(12)	0.036(6)
C(44)	0.1627(15)	0.1081(12)	1.1419(11)	0.032(5)
C(45)	0.0722(15)	0.2042(11)	1.1153(11)	0.029(5)
C(46)	0.0632(14)	0.2130(10)	1.0078(13)	0.032(5)

Table 6

Atomic coordinates and equivalent isotropic displacement parameters [Å^2] for 7. U_{eq} is defined as one third of the orthogonalized U_{ij} tensor

Atom	x	y	z	U_{eq}
Cr	0.23482(13)	−0.43987(11)	0.84000(8)	0.0269(3)
P	−0.1578(2)	−0.5077(2)	0.67570(13)	0.0262(5)
P'	0.3009(2)	−0.0976(2)	0.77818(13)	0.0252(5)
C(1)	0.0109(8)	−0.5374(7)	0.7236(5)	0.025(2)
C(2)	0.1172(8)	−0.4893(7)	0.6793(5)	0.031(2)
C(3)	0.2429(9)	−0.5181(7)	0.7058(5)	0.035(2)
C(4)	0.2633(9)	−0.6063(7)	0.7780(6)	0.038(2)
C(5)	0.1577(9)	−0.6596(7)	0.8209(6)	0.040(2)
C(6)	0.0320(9)	−0.6274(7)	0.7952(5)	0.033(2)
C(7)	−0.2699(9)	−0.6078(8)	0.7443(6)	0.050(2)
C(8)	−0.2492(9)	−0.6209(7)	0.5543(5)	0.040(2)
C(1')	0.3215(8)	−0.2193(6)	0.8629(5)	0.026(2)
C(2')	0.2130(8)	−0.2749(6)	0.9068(5)	0.025(2)
C(3')	0.2255(9)	−0.3674(7)	0.9752(5)	0.031(2)
C(4')	0.3469(8)	−0.4056(7)	1.0006(5)	0.033(2)
C(5')	0.4552(9)	−0.3488(8)	0.9592(6)	0.042(2)
C(6')	0.4428(6)	−0.2584(5)	0.8903(4)	0.033(2)
C(7')	0.4555(6)	0.0649(5)	0.8522(4)	0.042(2)
C(8')	0.3725(8)	−0.1275(7)	0.6843(5)	0.034(2)
Co(1)	−0.16418(11)	−0.29601(10)	0.65437(7)	0.0277(3)
Co(2)	0.07786(11)	−0.08437(9)	0.71776(7)	0.0250(3)
Co(3)	−0.10292(11)	−0.13835(10)	0.80414(7)	0.0290(3)
C(9)	−0.3076(8)	−0.3440(7)	0.5327(6)	0.033(2)
O(9)	−0.4008(6)	−0.3702(6)	0.4567(4)	0.055(2)
C(10)	0.0009(8)	−0.2335(7)	0.6070(5)	0.027(2)
O(10)	0.0306(6)	−0.2639(5)	0.5415(4)	0.0377(13)
C(11)	−0.2826(9)	−0.3162(9)	0.7310(6)	0.046(2)
O(11)	−0.3920(7)	−0.3805(6)	0.7425(5)	0.074(2)
C(12)	−0.1230(8)	−0.1026(7)	0.6702(5)	0.030(2)
C(12')	−0.2002(9)	−0.0255(8)	0.6061(5)	0.042(2)
C(13)	0.1193(9)	−0.0076(7)	0.8519(6)	0.030(2)
O(13)	0.2053(6)	0.0646(5)	0.9256(4)	0.0366(13)
C(14)	0.1373(10)	0.0562(8)	0.6575(5)	0.039(2)
O(14)	0.1750(7)	0.1456(6)	0.6149(4)	0.061(2)
O(16)	−0.2268(7)	0.0517(6)	0.8343(5)	0.060(2)
C(15)	−0.0754(9)	−0.2123(8)	0.9182(6)	0.039(2)
O(15)	−0.0656(7)	−0.2658(7)	0.9866(4)	0.067(2)
C(16)	−0.1780(9)	−0.0237(8)	0.8235(6)	0.039(2)

$+ (0.0495p)^2$ with $p = (F_0^2 + 2F_0^2)/3$: goodness-of-fit on $F^2 = 0.840$; max $\Delta\rho = 0.798$ e Å^{-3}.

References and notes

[1] Ch. Elschenbroich, A. Bretschneider-Hurley, J. Hurley, A. Behrendt, W. Massa, S. Wocadlo and E. Reijerse, Inorg. Chem., 34 (1995) 743.

[2] (a) N.G. Connelly and W.E. Geiger, Adv. Organomet. Chem., 23 (1984) 1; (b) W.E. Geiger and N.G. Connelly, Adv.

Organomet. Chem., 24 (1985) 87; (c) W.E. Geiger, A. Salzer, J. Edwin, W. von Philipsborn, U. Piantini and A.L. Rheingold, J. Am. Chem. Soc., 112 (1990) 7113 and preceding papers in the series; (d) W.E. Geiger, Progr. Inorg. Chem., 33 (1985) 275.

[3] D.E. Richardson and H. Taube, Coord. Chem. Rev., 60 (1984) 107.

[4] (a) K. Hinkelmann, J. Heinze, H.-T. Schacht, J.S. Field and H. Vahrenkamp, J. Am. Chem. Soc., 111 (1989) 5078; (b) A.J. Downard, B.H. Robinson and J. Simpson, Organometallics, 5 (1986) 1132 and preceding papers; (c) G.J. Bezems, P.H. Rieger and S. Visco, J. Chem. Soc., Chem. Commun., (1981) 265.

[5] Ch. Elschenbroich, G. Heikenfeld, M. Wünsch, W. Massa and G. Baum, Angew. Chem. Int. Ed. Engl., 27 (1988) 414.

[6] (a) S. Onaka, T. Moriya, S. Takagi, A. Mizuno and H. Furuta, Bull. Chem. Soc. Jpn., 65 (1992) 1415; (b) S. Onaka, M. Otsuka, A. Mizuno, S. Takagi, K. Sako and M. Otomo, Chem. Lett., (1994) 45; (c) T.-J. Kim, S.-C. Kwon, Y.-H. Kim and N.H. Heo, J. Organomet. Chem., 426 (1992) 71; (d) W.H. Watson, A. Nagl, S. Hwang and M.G. Richmond, J. Organomet. Chem., 445 (1983) 163.

[7] (a) T.W. Matheson, B.H. Robinson and W.S. Than, J. Chem. Soc. A (1971) 1457; (b) M.D. Brice, B.R. Penfold, B.H. Robinson and S.R. Taylor Inorg. Chem. 9 (1970) 362.

[8] Ch. Elschenbroich, T. Isenburg, B. Metz, A. Behrendt and K. Harms, J. Organomet. Chem., 481 (1994) 153.

[9] P.A. Dawson, B.H. Robinson and J. Simpson, J. Chem. Soc., Dalton Trans., (1979) 1762.

[10] A.J. Downard, B.H. Robinson and J. Simpson, Organometallics, 5 (1986) 1122.

[11] G. Balavoine, J. Collin, J.J. Bonnet and G. Lavigne J. Organomet. Chem., 280 (1985) 429.

[12] T.W. Matheson and R.B. Penfold, Acta Crystallogr. Sect. B: Struct. B 33 (1977) 1980.

[13] S. Aime, M. Botta, R. Gobetto and D. Osella, J. Organomet. Chem. 320 (1987) 229.

[14] B.R. Penfold and B.H. Robinson, Acc. Chem. Res., 6 (1973) 73.

[15] (a) H. Binder and Ch. Elschenbroich, Angew. Chem. Int. Ed.

Engl., 12 (1973) 659; (b) Ch. Elschenbroich S. Hoppe, and B. Metz, Chem. Ber., 126 (1993) 399; (c) Ch. Elschenbroich and U. Zenneck, J. Organomet. Chem., 160 (1978) 125.

[16] T.W. Matheson and B.H. Robinson, J. Organomet. Chem., 88 (1975) 367.

[17] Ch. Elschenbroich, E. Bilger and B. Metz, Organometallics, 10 (1991) 2823.

[18] K. Hinkelmann, F. Mahlendorf, J. Heinze, H.-T. Schacht, J.S. Field and H. Vahrenkamp, Angew. Chem. Int. Ed. Engl., 26 (1987) 352.

[19] A.M. Bond, P.A. Dawson, B.M. Peake, P.H. Rieger, B.H. Robinson and J. Simpson, Inorg. Chem., 18 (1979) 1413.

[20] (a) B.M. Peake, B.H. Robinson, J. Simpson and D.J. Watson, Inorg. Chem., 16 (1977) 405; (b) B.M. Peake, P.H. Rieger, B.H. Robinson and J. Simpson, Inorg. Chem., 18 (1979) 1000.

[21] See refs. 8–11 in Ref. [4a].

[22] Ch. Elschenbroich, M. Nowotny, J. Kroker, A. Behrendt, W. Massa and S. Wocadlo, J. Organomet. Chem., 459 (1993) 157.

[23] D. Seyferth, D. Hallgren and P.L.K. Hung, J. Organomet. Chem., 50 (1973) 265.

[24] (a) J. Kochi, J. Organomet. Chem. 300 (1986) 139; (b) J.K. Kochi, in W.C. Trogler (ed.), J. Organomet. Chem. Library, 22 (1990) 201, Organometallic Radical Processes, Chap. 7.

[25] D.S. Brown, M.-H. Delville-Desbois, R. Boese, K.P.C. Vollhardt and D. Astruc, Angew. Chem. Int. Ed. Engl., 33 (1994) 661.

[26] J. Sebbach, Dissertation, Marburg, 1991; Ch. Elschenbroich and J. Sebbach, unpublished observations, 1992.

[27] B. Olbricht-Deußner, R. Groß and W. Kaim, J. Organomet. Chem., 366 (1989) 155.

[28] Further details of the crystal structure investigation are available on request from the Fachinformationszentrum Karlsruhe, Gesellschaft für wissenschaftlich-technische Information mbH, D-76344 Eggenstein-Leopoldshafen (Germany) on quoting the depository numbers CSD 404113 (6) and CSD 404112 (7), the names of the authors, and the journal citation.